Brain Struct Funct (2016) 221:3157–3170
DOI 10.1007/s00429-015-1093-9

ORIGINAL ARTICLE

# Intertemporal choice behavior is constrained by brain structure in healthy participants and pathological gamblers

**Bahram Mohammadi[1,2] · Anke Hammer[1,3] · Stephan F. Miedl[4,7] · Daniel Wiswede[1,5] · Josep Marco-Pallarés[6] · Manfred Herrmann[7] · Thomas F. Münte[1,5]**

Received: 30 August 2014 / Accepted: 25 July 2015 / Published online: 4 August 2015


**Abstract** The steepness of the delay discounting function shows considerable interindividual differences. Moreover, faster devaluation of future rewards has been consistently observed in pathological gamblers (PGs). Here, we asked whether variability in delay discounting is at least partially driven by differences in the anatomy of gray and white matter. For 40 healthy young subjects (study 1) as well as 15 PG and 15 age-matched healthy controls (HCs, study 2), the individual discounting parameter $k$ was obtained. Based on 3D T1-weighted high-resolution magnetic resonance scans and diffusion tensor imaging, we performed voxel-based morphometry and tract-based spatial statistics, respectively, to examine the relation of gray matter volume (GMV) and white matter properties (as indicated by fractional anisotropy, FA) to $k$. Healthy groups from both studies showed a negative correlation between $k$ and FA for the superior longitudinal fascicle and inferior longitudinal fascicle, whereas a positive correlation was found in the PG group for the inferior longitudinal fascicle and left inferior fronto-occipital fascicle. The latter also was significantly different between HC and PG in the group statistics (albeit on the right side), thus suggesting that this is a significant structure for the development of pathological gambling. GMV of the right frontal orbital cortex, left insular cortex and right lateral occipital cortex showed a positive correlation to $k$ HC (studies 1 and 2) and PG, whereas a negative correlation was found for the left frontal pole in all three groups. Group comparison of GMV (study 2) revealed a decrease in PG for several cortical and subcortical areas.

**Keywords** Intertemporal choice · Delay discounting · Diffusion tensor imaging · Voxel-based morphometry · Pathological gambling · fMRI · Reward

**Abbreviations**

| | |
|---|---|
| DSM IV | Diagnostic and Statistical Manual IV |
| DTI | Diffusion tensor imaging |
| EPI | Echo planar imaging |
| FA | Fractional anisotropy |
| FOV | Field of view |
| FWHM | Full width half maximum |
| HC | Healthy control |
| KFG | Kurzfragebogen zum Glücksspielverhalten (German gambling questionnaire) |
| LDR | Large delayed reward |
| MR | Magnetic resonance |
| PG | Pathological gambler |
| SIR | Small immediate reward |
| SOGS | South Oaks Gambling Screen |
| TBSS | Tract-based spatial statistics |
| VBM | Voxel-based morphometry |

B. Mohammadi and A. Hammer contributed equally.

✉ Thomas F. Münte
Thomas.muente@neuro.uni-luebeck.de

1 Department of Neurology, University of Lübeck, Ratzeburger Allee 160, 23538 Lübeck, Germany

2 International Neuroscience Institute, Hannover, Germany

3 Department of Psychiatry, University of Erlangen, Erlangen, Germany

4 Institute of Psychology, University of Salzburg, Salzburg, Austria

5 Institute of Psychology II, University of Lübeck, Lübeck, Germany

6 Institut d'Investigació Biomèdica de Bellvitge (IDIBELL), Barcelona, Spain

7 Department of Neuropsychology and Behavioral Neurobiology, University of Bremen, Bremen, Germany

## Introduction

To forego a small but immediate reward to attain a larger reward in the distant future is an important capacity of humans and, to a lesser extent, animals (Amiez et al. 2006; Kalenscher et al. 2005; Kalenscher and Pennartz 2008). Abstaining from consumption of immediate rewards is ultimately the basis of planning for the future, economic growth and individual progress. Intertemporal choice behavior has thus attracted the interest of economists (Frederick et al. 2003) and more recently cognitive neuroscientists (Peters and Büchel 2011). People differ considerably in their intertemporal choice behavior, some showing frequent impulsive choices for the immediately available reward, whereas others are willing to wait for the later reward. In addition to variation in the normal population (Anokhin et al. 2011), impulsive choices in intertemporal choice paradigms have also been observed in smokers (Reynolds et al. 2004; Mitchell 1999), alcoholics (Petry 2001a; Mitchell et al. 2005), heroin addicts (Kirby et al. 1999), patients with Parkinson's disease receiving dopaminergic medication (Milenkova et al. 2011), and pathological gamblers (PGs) (Alessi and Petry 2003; Dixon et al. 2003, 2006; Petry 2001b).

The decision in intertemporal choice paradigms can be viewed as the outcome of a competition between two cognitive and—by extension—neurobiological processes: one process mediates the urge to retrieve rewards whereas the second opposing process implements top-down control and may overrule the reward-seeking process to wait for a later greater reward (McClure et al. 2004). Research in behavioral economics in both, humans and animals (Frederick et al. 2002; Mazur 1984), has shown that the discounting of the delayed reward approximately follows a hyperbolic function:

$$V = \frac{A}{1 + kD},$$

where $V$ is the present value of the delayed reward $A$ after a delay $D$, and $k$ is the delay discount rate. A higher delay discount rate indicates a steeper discount function, i.e., a more pronounced devaluation of future rewards.

In the present investigation, we are concerned with individual differences in intertemporal choice. In particular, we ask to what extent such differences may be grounded in individual differences in brain anatomy. Gray matter anatomy was assessed on the basis of high-resolution T1-weighted MR images. In addition, the microstructure of white matter was characterized by fractional anisotropy (FA) derived from diffusion tensor magnetic resonance imaging (DTI) (Beaulieu 2002). Previous investigations have suggested that FA mirrors axonal microstructure in vivo (e.g., axon size, extent of myelination) (Basser and Jones 2002). It may thus be used to describe the quality of axonal connectivity (Waxman and Bennett 1972), which in turn might constrain the activity within the connected brain regions.

Individual differences in intertemporal choice were captured by the delay discounting rate $k$ (see equation given above) which was estimated from a series of choices following a method described by Kirby (Kirby et al. 1999). In study 1, 40 normal volunteers were studied and the relationship between $k$ and gray and white matter anatomy was assessed. In study 2, we compared 15 PGs, diagnosed according to DSM IV criteria, and 15 matched healthy control participants (HCs). Here, in addition to a group comparison of gray and white matter, we also performed correlation analyses involving the delay discount rate. Prior studies have shown that PG show steeper discounting of future rewards in laboratory settings (Alessi and Petry 2003; Dixon et al. 2003) as well as in more naturalistic tasks (Petry 2001b; Dixon et al. 2006) suggesting that impulsive discounting is one facet of the psychopathology in pathological gambling (see Wiehler and Peters 2014, for review).

The present investigation both replicates and extends previous studies (Yip et al. 2013; Koehler et al. 2013; Joutsa et al. 2011) on brain morphology and pathological gambling, as previous studies have only used a direct comparison between PG and HC groups and have not taken a measure of impulsivity (in our case the discount rate $k$) into account.

We expected to replicate the results of Joutsa et al. (2011); Yip et al. (2013) and Koehler et al. (2013) in the group comparison PG vs. HC in study 2, i.e., we expected to see lower fractional anisotropy in the PG in the corpus callosum, the cingulum, the superior longitudinal fascicle, the inferior fronto-occipital fascicle, the anterior limb of internal capsule, the anterior thalamic radiation, the inferior longitudinal fascicle and the uncinate/inferior fronto-occipital fascicle. The main focus of the current study was on the correlation between discount rate $k$ and gray matter density on the one hand and white matter integrity, however, as these correlations should pinpoint brain regions responsible for differences in intertemporal choice and therefore impulsivity more clearly than a group comparison. Based on recent findings by Peper et al. (2013) who found lower integrity (i.e., lower FA) in the frontostriatal tract in young healthy adults with faster discounting, we expected FA of the frontostriatal tract to correlate with $k$ in the present study. This expectation is also based on functional imaging studies that have shown increased activation of the striatum when participants choose immediate rewards over delayed rewards (e.g., McClure et al. 2004) on the one hand and greater activation of the prefrontal cortex in decisions for delayed rewards on the other hand

(e.g., Peters and Büchel 2011). We further expected that at least some of the white matter tracts that differed between PG and HC by Joutsa et al. (2011) to show a relationship to the individual discount rate.

## Methods

### Participants

A convenience sample of 40 healthy, right-handed students (11 women, mean age 24, range 18–29 years) participated in study 1 after giving informed consent. They were originally recruited for 2 different functional imaging studies on memory processes not related to the present study and performed the intertemporal choice task described below in addition and outside the scanner. They were assessed with the German gambling questionnaire "Kurzfragebogen zum Glücksspielverhalten" (KFG; derived from 20 items as developed by "Gamblers Anonymous") (Petry 1996). This questionnaire contains 20 items (4-point Likert scale: 0–3 points) addressing lifetime gambling behavior. The threshold for pathological gambling is set at 16 points. Participants of study 1 scored between 0 and 10 (mean 4.2 SD 2.9). Further, these participants were required to have no current or previous history of psychiatric or neurological diseases.

For study 2, 15 right-handed male PG (age 36.7, range 27–47 years) and 15 right-handed male HC (age 36.8, range 28–44 years) were recruited. None of the HC participants had participated in study 1. The PG group was recruited from various sources including a local counseling platform (http://www.gluecksspielsucht.uni-bremen.de/), word of mouth and a subject pool used in previous studies of the authors (Miedl et al. 2010). PG and HC did not differ in age ($t[14] = 0.18$, $p = 0.86$), smoking behavior ($t[14] = -0.43$, $p = 0.67$), income per month ($t[14] = -0.32$, $p = 0.75$) and years of education ($t[14] = 1.07$, $p = 0.30$, see Table 1). Prior to enrollment in the study, all participants underwent a structured psychiatric interview (SKID-I, Wittchen et al. 1997) and were familiarized with the experimental environment. To rule out psychopathological behavior which directly interferes with forced choice decision making, participants presenting a history of regular drug/alcohol abuse and psychotropic medication were excluded from the study. No active Axis I disorders (except for pathological gambling in PG) were present. Only men were assessed in study 2 as the prevalence of pathological gambling is two times higher in men than in women (Grant and Potenza 2004). The percentage of income spent on gambling activities was significantly higher in PG compared to HC ($t[14] = -2.65$, $p = 0.02$; see Table 1). In the PG group, all participants had a diagnosis of pathological gambling ($\geq$5 criteria) according to DSM IV. With regard to the KFG, all PG scored between 21 and 43 points, whereas HC scored between 0 and 16 points. In addition, all participants were evaluated with a German version of the South Oaks Gambling Screen (SOGS) (Lesieur and Blume 1987). All PG scored $\geq$6 on the SOGS, and HC obtained $\leq$4. Both groups significantly differed with respect to DSM IV ($t[14] = -12.55$, $p < 0.001$), SOGS ($t[14] = -11.14$, $p < 0.001$) and KFG scores ($t[14] = -12.08$, $p < 0.001$; Table 1). To summarize, PG and HC groups were matched for age, years of education, income, smoking and drinking behavior and absence of mood disorders but not for nutritional status. The study protocol complied with the Code of Ethics of the World Medical Association (Declaration of Helsinki 1984) and was approved by the local ethics committee. All participants were informed about the procedure and gave written informed consent to participate.

### Paradigm

A version of the monetary-choice task devised by Kirby (Kirby et al. 1999) was used. While the intertemporal choice task used in the present study is not a gambling task (as the participants had the choice between two sure rewards available at different points in time), it has been pointed out that steeper delay discounting functions are at

**Table 1** Demographic data of participants of study 2

| | PG ($n = 15$) | Control ($n = 15$) | |
|---|---|---|---|
| Age | 36.7 ± 5.8 | 36.8 ± 5.6 | $t[14] = 0.18$, $p = 0.86$ |
| cigarettes per day | 14 ± 11.2 | 12.4 ± 7.7 | $t[14] = -0.43$, $p = 0.67$ |
| Alcoholic drinks per day | 1.17 ± 1.75 | 1.29 ± 1.81 | $t[14] = -0.19$, $p = 0.857$ |
| DSM IV | 6.8 ± 1.8 | 0.3 ± 0.6 | $t[14] = -12.55$, $p < 0.001$ |
| SOGS | 10.9 ± 2.8 | 0.8 ± 1.3 | $t[14] = -11.14$, $p < 0.001$ |
| KFG | 34.1 ± 7.6 | 2.7 ± 4.5 | $t[14] = -12.08$, $p < 0.001$ |
| Income spent on gambling (%) | 82.1 ± 116 | 2.4 ± 3 | $t[14] = -2.65$, $p = 0.02$ |
| Net income in € per month | 1533 ± 823 | 1450 ± 642 | $t[14] = -0.32$, $p = 0.75$ |
| Years of education | 15.5 ± 2.7 | 16.1 ± 3.1 | $t[14] = 1.07$, $p = 0.30$ |

the core of the psychopathology of PG (see, for example, the recent review by Wiehler and Peters 2014). Because of the non-gambling character of the task, we deemed it ethically justifiable to test PG participants with this task.

In study 1, participants were confronted with 27 decisions (Table 2) in a paper and pencil format. Each decision involved the choice between a small immediate reward (SIR) and a larger delayed reward (LDR). The order of trials was arranged such that the trial order did neither correlate with the SIR or LDR amounts, nor with the temporal difference, delay or the discounting rate. Participants were instructed to make each decision as if it was real. To provide an incentive to do so, they were informed that following the questionnaire they would be allowed to throw a dice. If they managed to obtain a score of 6 they were allowed to draw a number between 1 and 27 (each standing for one decision). They would then receive a reward according to their actual choice on that trial. If the participant had chosen the SIR he was given cash corresponding to the SIR, if the participant had chosen the LDR he was to receive the particular sum via bank transfer after the appropriate delay. Of the 40 participants, 8 obtained a score of 6 upon throwing the dice and received a reward. All others only received 16 € for participation in the scanning session.

In study 2, the choices were presented during a functional MRI session following the method developed by Marco-Pallares et al. (Marco-Pallares et al. 2010). Here, participants took part in 4 runs, each with a fixed set of 27 choices. Again, the order of trials within each run was arranged such that the trial order did neither correlate with the SIR or LDR amounts, nor with the temporal difference, delay or the discounting rate. Each trial began with a fixation cross (+) that lasted 8 s followed by the two choices

**Table 2** Choices presented in the delay discounting task in study 1

| | Order | SIR | LDR | Delay (days) | *K* indiff | *K* rank | LDR size |
|---|---|---|---|---|---|---|---|
| 1 | 13 | € 34 | € 35 | 186 | 0.00016 | 1 | S |
| 2 | 1 | € 54 | € 55 | 117 | 0.00016 | 1 | M |
| 3 | 9 | € 78 | € 80 | 162 | 0.00016 | 1 | L |
| 4 | 20 | € 28 | € 30 | 179 | 0.0004 | 2 | S |
| 5 | 6 | € 47 | € 50 | 160 | 0.0004 | 2 | M |
| 6 | 17 | € 80 | € 85 | 157 | 0.0004 | 2 | L |
| 7 | 26 | € 22 | € 25 | 136 | 0.001 | 3 | S |
| 8 | 24 | € 54 | € 60 | 111 | 0.001 | 3 | M |
| 9 | 12 | € 67 | € 75 | 119 | 0.001 | 3 | L |
| 10 | 22 | € 25 | € 30 | 80 | 0.0025 | 4 | S |
| 11 | 16 | € 49 | € 60 | 89 | 0.0025 | 4 | M |
| 12 | 15 | € 69 | € 85 | 91 | 0.0025 | 4 | L |
| 13 | 3 | € 19 | € 25 | 53 | 0.006 | 5 | S |
| 14 | 10 | € 40 | € 55 | 62 | 0.006 | 5 | M |
| 15 | 2 | € 55 | € 75 | 61 | 0.006 | 5 | L |
| 16 | 18 | € 24 | € 35 | 29 | 0.016 | 6 | S |
| 17 | 21 | € 34 | € 50 | 30 | 0.016 | 6 | M |
| 18 | 25 | € 54 | € 80 | 30 | 0.016 | 6 | L |
| 19 | 5 | € 14 | € 25 | 19 | 0.041 | 7 | S |
| 20 | 14 | € 27 | € 50 | 21 | 0.041 | 7 | M |
| 21 | 23 | € 41 | € 75 | 20 | 0.041 | 7 | L |
| 22 | 7 | € 15 | € 35 | 13 | 0.1 | 8 | S |
| 23 | 8 | € 25 | € 60 | 14 | 0.1 | 8 | M |
| 24 | 19 | € 33 | € 80 | 14 | 0.1 | 8 | L |
| 25 | 11 | € 11 | € 30 | 7 | 0.25 | 9 | S |
| 26 | 27 | € 20 | € 55 | 7 | 0.25 | 9 | M |
| 27 | 4 | € 31 | € 85 | 7 | 0.25 | 9 | L |

*SIR* small immediate reward, *LDR* large delayed reward, *K* indiff delay discounting value at which the two decisions are of equal subjective value, *K rank* trials were ranked according to *K* indiff into 9 classes, *LDR size* the size of the delayed reward was classified as small (S, between 25 and 35€), medium (M, between 50 and 60€) and large (L, between 75 and 85€). In study 2, four sets of similarly constructed choices were presented in four runs of functional imaging

which were displayed while the cross was continuously present (e.g., "55€ heute + 57€ in 117 Tagen", "55€ today + 57€ after 117 days"). The participant had to choose the preferred option by pressing one of two buttons on an MR-compatible response pad. Each participant received 16 € for participation.

As in study 1, to provide an incentive to perform the decisions as if they were real, participants were informed prior to the experiment that after the experiment they would receive the outcome of one of their 108 decisions. Participants were allowed to draw a trial number after the experiment was finished and their decision on that particular trial was derived from the log-files of the experiment. If the participant had chosen the immediate reward, he received the sum in cash, in case of a choice for the delayed reward the sum was transferred to the participant's bank account after the appropriate delay period.

The computation of individual discounting rate parameter ($k$-rate) was performed as described by Kirby et al. (Kirby et al. 1999), assigning a $k$ value to each subject that produces the highest proportion of choices consistent with that $k$ value. For example, a participant with a $k$-rate coinciding with the $k$ of a certain choice would be indifferent to this selection. For example, if s/he had a $k$ of 0.001, s/he would be indifferent to the selection of 67€ now or 75€ in 119 days (Table 2). If s/he had a greater individual $k$-rate, s/he would select the immediate reward. Then, choices with the next $k$ value were examined (i.e., 49€ now or 60€ in 89 days, corresponding to $k = 0.0025$). If the participant selected the delayed reward in this case, the individual $k$ was calculated to be the geometric mean of the two $k$ values, that is 0.0016.

We also computed the consistency of $k$ (percentage of participant's choices that were consistent with their assigned discount rate) over all trials to ensure that it reflected the general behavior of participants and that it was consistent across the different runs.

## Image acquisition

Study 1: MRI data were recorded using a 3 T SIEMENS Magnetom Trio whole body scanner (Siemens, Erlangen, Germany) equipped with a 32 channel head coil. Conventional high-resolution structural images [magnetization-prepared, rapid-acquired gradient echoes (MPRAGE) sequence, 192 slice sagittal, TR = 2500 ms, TE = 4.77 ms, TI = 1100 ms, flip angle = 7°, 1 mm thickness (isotropic voxels)] were recorded for anatomical reference.

DTI data were collected employing a diffusion tensor spin-echo EPI sequence. Diffusion weighting was conducted using the pulsed-gradient spin-echo (PGSE) method. Images were measured using 2-mm-thick slices, no gap, TR = 4200 ms, TE = 74 ms, 128 × 128 acquisition matrix and subsequently interpolated by zero padding to 256 × 256 to allow co-registration with the T1 data set. The FOV was 28 cm and 64 axial slices were obtained. To obtain diffusion tensors, diffusion was measured along 12 directions ([Gx,Gy,Gz] = [1.0,0.0,0.5], [0.0,0.5,1.0], [0.5,1.0,0.0], [1.0,0.5,0.0], [0.0,1.0,0.5], [0.5,0.0,1.0], [1.0,0.0,−0.5], [0.0,−0.5,1.0], [−0.5,1.0,0.0], [1.0,−0.5,0.0], [0.0,1.0,−0.5], [−0.5,0.0,1.0]) chosen according to the DTI acquisition scheme proposed by (Papadakis et al. 1999), and the values specified by (Skare et al. 2000) using a single $b$ value of 1000 s/mm$^2$. Unipolar gradients were used. Three runs were acquired per slice and diffusion gradient direction.

Study 2: Data were obtained with a 3 T Siemens Magnetom Allegra head scanner that uses a whole-head, local-gradient coil. A T1-weighted structural 3D image of the brain was obtained using the MPRAGE sequence: 176 contiguous slices, TR = 2.3 s, TE = 4.38 ms, TI = 900 ms, FA = 8°, FOV 256 × 256 mm, in-plane resolution 1 × 1 mm, slice thickness 1 mm.

Diffusion weighting was conducted using the twice-refocused PGSE method. Images were measured using 2-mm-thick slices, no gap, TR = 8100 ms, TE = 85 ms, 128 × 128 acquisition matrix, interpolated by zero padding to 256 × 256, FOV 28 cm, 64 axial slices. To obtain diffusion tensors, diffusion was measured along 30 directions using a single $b$ value of 1000 s/mm$^2$. Four runs were acquired per slice and diffusion gradient direction. Unipolar gradients were used.

## Voxel-based morphometry (VBM)

Structural data were analyzed with FSL-VBM, a voxel-based morphometry style analysis (Ashburner and Friston 2000; Good et al. 2001) carried out with FSL tools (Smith et al. 2004). First, structural images were brain-extracted using the BET tool (Smith 2002) which deletes non-brain tissue from an image of the whole head. Next, tissue-type segmentation was carried out using FAST4 (Zhang et al. 2001), which segments a 3D image of the brain into different tissue types (gray and white matter, CSF) and corrects for spatial intensity variations. The resulting gray matter partial volume images were then aligned to MNI152 standard space using FLIRT (Jenkinson and Smith 2001; Jenkinson et al. 2002) which is a fully automated tool for linear (affine) brain image registration. This was followed by nonlinear registration using FNIRT (Andersson et al. 2007a, b), which uses a b-spline representation of the registration warp field (Rueckert et al. 1999). The resulting images were averaged to create a study-specific template, to which the native gray matter images were then non-linearly re-registered. The registered partial volume images were then modulated (to correct for local expansion or

contraction) by dividing by the Jacobian of the warp field. The modulated segmented images were then smoothed with an isotropic Gaussian kernel with a sigma of 3 mm (corresponding to a 7-mm FWHM). Finally, voxelwise GLM was applied using permutation-based non-parametric testing (5000 permutations). The resulting maps were thresholded at $p < 0.05$ (Family-wise error corrected; FWE) using threshold-free cluster enhancement (TFCE) to define clusters of significant changes (Smith and Nichols 2009). TFCE has been developed to avoid the problem of selecting a cluster-forming threshold in topological inference procedures. This is achieved by integrating excursion sets over all the possible thresholds thus resulting in a new set of values reflecting cluster height and support. The FWE correction was implemented as described by Smith and Nichols (2009).

Correlations between $k$ and gray matter volume were performed for all voxels in the gray matter images.

Data were visualized in MNI standard space.

### Tract-based spatial statistics (TBSS)

Voxelwise statistical analysis of the FA data was carried out using TBSS [Tract-Based Spatial Statistics, (Smith et al. 2006)], part of FSL (Smith et al. 2004). First, FA images were created by fitting a tensor model to the raw diffusion data using FDT (FSL diffusion toolbox allowing for eddy current distortion correction, modeling of diffusion parameters and local fitting of diffusion tensors), and then brain-extracted using BET (Smith 2002). All subjects' FA data were then aligned into a common space using the nonlinear registration tool FNIRT. Next, the mean FA image was created and thinned to create a mean FA skeleton which represents the centers of all tracts common to the group. Each subject's aligned FA data were then projected onto this skeleton and the resulting data fed into voxelwise cross-subject statistics. Likewise, correlations between $k$ and FA were performed for all voxels in the FA skeleton. We used permutation-based non-parametric testing (5000 permutations). The resulting maps were thresholded at $p < 0.05$ (FWE) using TFCE to define clusters of significant changes.

Data were visualized in MNI standard space using FSLView.

## Results

### Intertemporal choice behavior

In study 1, the delay discount value was $0.03 \pm 0.09$. The consistency (percentage of participant's choices that were consistent with their assigned discount rate) was $96 \pm 4$ %. There were no differences between women and men with regard to $k$.

For study 2, across all reward magnitudes, the mean $k$ was $0.06 \pm 0.08$ for the PG and $0.02 \pm 0.03$ for the HC. For statistical testing ($t$ test), the distributions of the $k$ values of PG and HC were normalized using the natural log transformation. There was a reliable difference between the groups, $t(28) = 2.6$, $p = 0.015$, Cohen's $d = 0.98$. The consistency (percentage of participant's choices that were consistent with their assigned discount rate) was $96 \pm 4$ % (PG: $95 \pm 4$ %; HC: $96 \pm 4$ %) over all 4 runs. There were no significant differences between groups in consistency across the different runs (HC: 1st run: $95 \pm 6$ %; 2nd run: $96 \pm 3$ %, 3rd run: $94 \pm 5$ %, 4th run: $95 \pm 5$ %; PG: run: $98 \pm 4$ %; 2nd run: $97 \pm 4$ %, 3rd run: $95 \pm 6$ %, 4th run: $95 \pm 5$ %; $F(3,84) = 3.4$, $p > 0.7$).

### Voxel-based morphometry

Study 1: The discount rate $k$ showed a positive correlation with gray matter volume in the superior division of right lateral occipital cortex, left insular cortex and right frontal orbital cortex. A negative correlation was found for the left frontal pole (Fig. 1; Table 3).

Study 2: Comparing both groups, a decreased gray matter volume in PG was revealed for the anterior cingulate gyrus (right), the frontoorbital cortex (right), the precentral gyrus (right) and the insula (right), the bilateral supplemental motor area, the bilateral putamen, and the right amygdala and hippocampus (Fig. 2; Table 4). There was no significant reduction of gray matter density in HC compared to PG.

The $k$ value showed a significant correlation with gray matter volume in different areas in the entire sample (HC and PG combined) as well as in HC and PG (Fig. 3; Table 5). For the entire group, a positive correlation was revealed between $k$ and gray matter volume in right and left

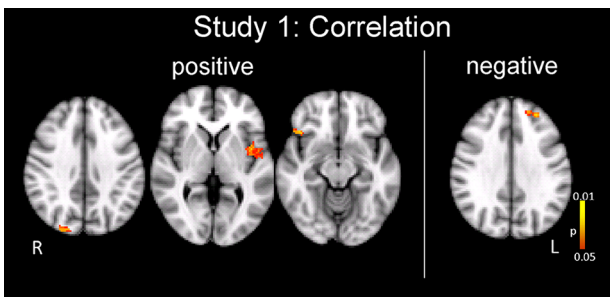


**Fig. 1** Study 1: VBM-style analysis showing correlations of gray matter density to the individual discounting rate $k$; TFCE, FWE corrected ($p < 0.05$). A positive correlation was observed for the right lateral occipital cortex, superior division, left insular cortex and right frontal orbital cortex. A negative correlation was revealed for the left frontal pole (superior frontal gyrus)

**Table 3** Study 1: VBM-style analysis showing brain regions correlating with *k* value

| Brain region | Hemisphere | MNI coordinates | | | Cluster size | *p* (FWE) |
|---|---|---|---|---|---|---|
| | | *X* | *Y* | *Z* | | |
| Positive correlation | | | | | | |
| Lateral occipital cortex, superior division | R | 18 | −86 | 28 | 575 | 0.01 |
| Insular cortex | L | −42 | −4 | 0 | 222 | 0.02 |
| Frontal orbital cortex | R | 42 | 22 | −10 | 87 | 0.01 |
| Negative correlation | | | | | | |
| Frontal pole, superior frontal gyrus | L | −28 | 54 | 30 | 124 | 0.02 |

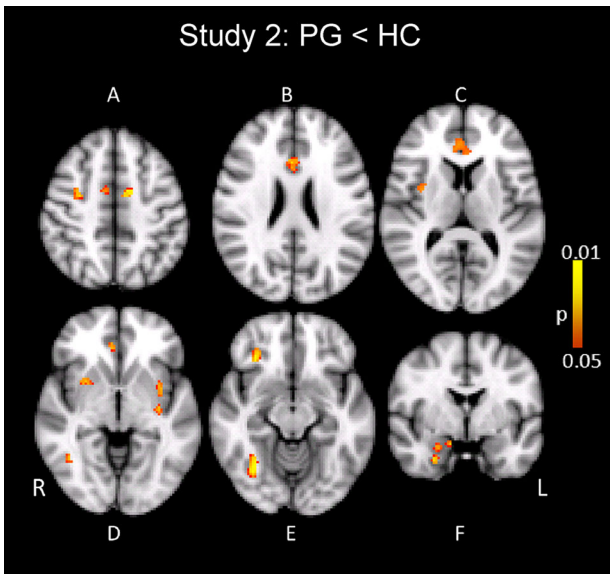


**Fig. 2** Study 2: Voxel-based morphometry (TFCE, FWE corrected, $p < 0.05$) showed regions of decreased gray matter density in PG in the bilateral SMA and right precentral gyrus (**a**), the cingulate gyrus (**b**, **c**), the right insula (**c**), the bilateral putamen, right insula and right inferior temporal gyrus (**d**), the right frontal orbital cortex and right fusiform gyrus (**e**), right amygdala and right hippocampus (**f**)

frontoorbital cortex as well as in the left insula. For HC, we found a positive correlation of *k* and gray matter volume in right frontal orbital cortex, left insular cortex and right lateral occipital cortex. PG showed a positive correlation between *k* and gray matter volume for the left insular cortex, right lateral occipital cortex and the left frontal orbital cortex. A negative correlation between *k* value and gray matter of the left frontal pole (superior frontal gyrus) emerged for the entire group as well as for both groups separately.

## DTI results

Study 1: Using DTI images and TBSS analysis, we found a significant negative correlation between FA and *k* value (Fig. 4; Table 6) in the left superior longitudinal fascicle, right inferior longitudinal fascicle and left inferior longitudinal fascicle. Testing for positive correlations showed no significant results.

Study 2: Figure 5 shows those parts of white matter tracts with a significantly reduced FA in PG compared to HC (Table 7). These included the superior longitudinal fascicle (bilateral), left inferior longitudinal fascicle, right

**Table 4** Study 2: Regions with decreased gray matter intensity in PG compared to HC evaluated with VBM

| Brain region | Hemisphere | MNI coordinates | | | Cluster size | *p* (FWE) |
|---|---|---|---|---|---|---|
| | | *X* | *Y* | *Z* | | |
| Cingulate gyrus, anterior division | R | 2 | 20 | 24 | 190 | 0.02 |
| Putamen | R | 24 | 4 | 0 | 152 | 0.01 |
| Frontal orbital cortex | R | 32 | 30 | −12 | 102 | 0.03 |
| Amygdala | R | 16 | −4 | −20 | 100 | 0.02 |
| Precentral gyrus | R | 28 | −8 | 44 | 95 | 0.01 |
| Insular cortex | R | 34 | 0 | 12 | 90 | 0.04 |
| Hippocampus | R | 20 | −14 | −20 | 89 | 0.02 |
| SMA | L | −12 | −4 | 48 | 71 | 0.01 |
| SMA | R | 12 | 0 | 46 | 69 | 0.02 |
| Putamen | L | −32 | −14 | 0 | 68 | 0.02 |
| Inferior temporal gyrus | R | 42 | −58 | −6 | 44 | 0.04 |
| Insular cortex | L | −38 | 0 | −6 | 43 | 0.04 |
| Occipital fusiform gyrus | R | 40 | −64 | −14 | 28 | 0.04 |

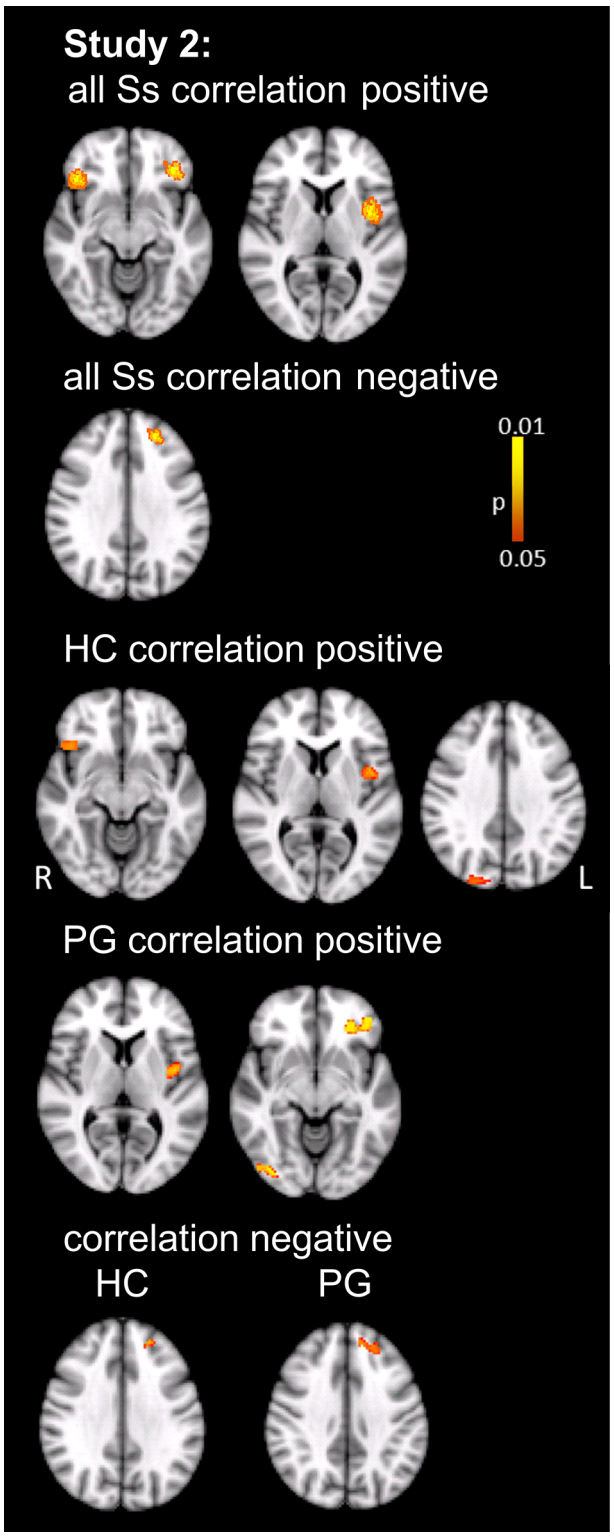


**Fig. 3** Study 2: Similar areas showed positive correlations between gray matter density and discounting rate $k$ in HC (*upper row*) and PG (*middle row*). Likewise, areas showing negative correlations were similar in HC and PG (*lower row*). TFCE, FWE corrected, $p < 0.05$

inferior fronto-occipital fascicle and the bilateral anterior thalamic radiation. There were no areas with a significant reduction of FA in HC compared to PG.

When correlations between $k$ and FA were assessed for the entire group, no area passed the statistical threshold. By contrast, when both groups were assessed separately, discounting rate $k$ and FA were negatively correlated in several regions including the left superior longitudinal fascicle as well as the bilateral inferior longitudinal fascicle in HC, whereas in PG a positive correlation was revealed for the left inferior fronto-occipital fascicle and the left superior longitudinal fascicle (Fig. 6; Table 8).

## Discussion

In the present study, we sought to delineate anatomical regions, both in gray and white matter, that are related to decision making in intertemporal choice. In addition to healthy participants, we also investigated PG to see whether the same relations between intertemporal choice behavior and interindividual anatomical differences hold for HC and PG and to look for general morphological differences between PG and controls.

Behaviorally, we could replicate numerous studies (reviewed, e.g., in Wiehler and Peters 2014) that have shown a steeper delay discounting function in PG. Wiehler and Peters (2014) hypothesized that PG are associated with impulsive choice behavior, as measured with the DD paradigm, in a rather categorical manner, as studies looking for a correlation between addiction severity and $k$ did not find such an association (e.g., Alessi and Petry 2003; Brevers et al. 2012; Kräplin et al. 2014; Miedl et al. 2012). As delay discounting behavior in PG is related to questionnaire measures of impulsivity (e.g., Alessi and Petry, 2003; Kräplin et al. 2014, a steeper delay discounting might be interpreted as a behavioral marker underlying both impulsive behavior and pathological gambling in particular.

### Regions related to intertemporal choice

Steeper discounting of future rewards is an important aspect of psychopathology in pathological gambling (Alessi and Petry 2003; Dixon et al. 2003, 2006; Petry 2001b; Wiehler and Peters 2014). We therefore were interested whether cortical brain regions as well as white matter tracts could be identified, which show a relation to the individual delay discounting rate as estimated by parameter $k$.

With regard to gray matter volume, a positive correlation with $k$ was found in the right frontal orbital cortex, left

**Table 5** Study 2: Regions showing a significant correlation between gray matter intensity and *K* value in HC and PG

| Brain region | Hemisphere | MNI coordinates | | | Cluster size | *p* (FWE) |
|---|---|---|---|---|---|---|
| | | *X* | *Y* | *Z* | | |
| Entire sample positive correlation | | | | | | |
| Frontal orbital cortex | R | 40 | 34 | −14 | 132 | 0.01 |
| Frontal orbital cortex | L | −36 | 36 | −14 | 254 | 0.01 |
| Insular cortex | L | −38 | −4 | 6 | 202 | 0.01 |
| HC positive correlation | | | | | | |
| Lateral occipital cortex, superior division | R | 24 | −88 | 24 | 415 | 0.01 |
| Insular cortex | L | −40 | 0 | −2 | 173 | 0.01 |
| Frontal orbital cortex | R | 38 | 32 | −12 | 79 | 0.01 |
| PG positive correlation | | | | | | |
| Frontal orbital cortex | L | −34 | 38 | −16 | 292 | 0.01 |
| Insular cortex | L | −34 | −6 | 10 | 230 | 0.03 |
| Lateral occipital cortex, inferior division | R | 36 | −84 | −8 | 152 | 0.01 |
| Entire sample negative correlation | | | | | | |
| Frontal pole, superior frontal gyrus | L | −20 | 44 | 32 | 198 | 0.01 |
| HC negative correlation | | | | | | |
| Frontal pole, superior frontal gyrus | L | −18 | 44 | 28 | 33 | 0.04 |
| PG negative correlation | | | | | | |
| Frontal pole, superior frontal gyrus | L | −20 | 44 | 44 | 117 | 0.02 |

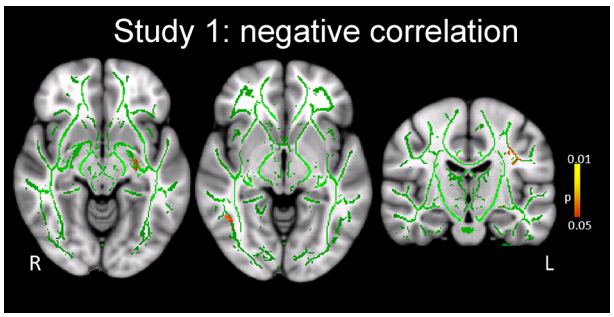


**Fig. 4** Study 1: Voxelwise TBSS analysis; TFCE, FWE corrected ($p < 0.05$). Background image is the standard MNI template in FSL. The green voxels represent the mean FA skeleton, i.e., the centers of the tracts common to the group. *Red/yellow* voxels represent regions in which FA showed a significant negative correlation to *k* value. Such correlations were seen for the left superior longitudinal fascicle, right inferior longitudinal fascicle and left Inferior longitudinal fascicle

insular cortex and right lateral occipital cortex in the healthy subjects of study 1. For the entire sample of study 2, this pattern was basically replicated with positive correlations between *k* and gray matter volume in right and left frontoorbital cortex as well as in the left insula. When both groups were examined separately, HC showed a positive correlation for the right frontal orbital cortex, left insular cortex and right lateral occipital cortex. The PG participants of study 2 again showed a very similar pattern with positive correlations between *k* and left insular cortex, as well as right lateral occipital cortex volume. Again, a consistent picture emerged in volumes of brain areas demonstrating a negative correlation with *k* values, as the left frontal pole was the only region identified in this analysis in the healthy subjects of study 1, as well as in the entire sample of study 2 and HC and PG groups separately. These results partially replicate a recent VBM study on 34 healthy participants who were also subjected to a delay discounting task similar to the present one (Cho et al. 2013). In this study, a positive correlation between gray matter volume and *k* was obtained for the bilateral medial frontal gyrus, right orbitofrontal gyrus, bilateral anterior cingulate gyrus and left middle cingulate gyrus. Thus, the orbitofrontal cortex shows a consistent relationship to

**Table 6** Study 1: Areas showing a negative correlation between FA and discounting rate *k*

| Brain region | Hemisphere | MNI coordinates | | | Cluster size | *p* (FWE) |
|---|---|---|---|---|---|---|
| | | *X* | *Y* | *Z* | | |
| Superior longitudinal fascicle | L | −35 | −19 | 35 | 324 | 0.01 |
| Inferior longitudinal fascicle | R | 46 | −56 | −6 | 52 | 0.01 |
| Inferior longitudinal fascicle | L | −26 | −9 | −10 | 55 | 0.02 |

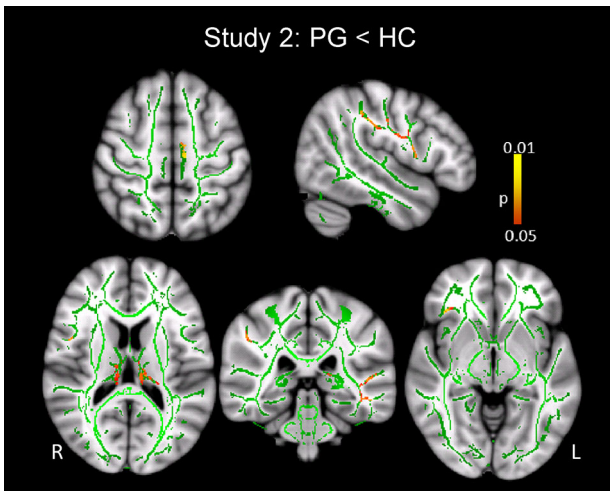


**Fig. 5** Study 2: White matter structures showing a significant decrease of FA in PG relative to HC (*red/yellow* voxels). The *green* voxels show the mean FA skeleton representing the centers of all of the tracts common to the group

*k* over 4 independent groups of participants. With regard to areas showing negative correlations to *k*, Cho et al. (2013) identified the bilateral ventral putamen, while the current data suggest the left frontal pole to be an important area. Whereas Cho et al. (2013) pointed out that these interindividual anatomical differences could be important for the emergence of pathological impulse control behaviors, the current study shows that at least for PGs a relationship between anatomical differences in frontal cortical areas and impulsivity exists.

The orbitofrontal cortex, showing a consistent positive correlation to *k* over our three groups, has been implicated in decoding and representing primary reinforcers, in learning and reversing associations of stimuli to these reinforcers as well as in controlling reward-related behaviors (Rolls 2004). It thus seems that a greater volume of this structure is associated with a steeper discounting function, i.e., a tendency to go for the smaller immediately available reward. Likewise, the left insular cortex emerged in all three groups as showing a positive relationship to *k* values. Numerous studies link the insula to impulsive behavior (Kuhnen and Knutson 2005a, b; Preuschoff et al. 2008; Xue et al. 2010) indicating that increased impulsivity might be an underlying problem for both pathological gambling and delay discounting (Wiehler and Peters 2014).

With regard to white matter tracts, again a consistent picture emerged regarding the participants of study 1 and the HC group of study 2 as significant negative correlations between FA and *k* were observed in the left superior longitudinal fascicle and the bilateral inferior longitudinal fascicle and left inferior longitudinal fascicle in both groups. No white matter region showed a positive correlation between FA and *k* in these groups. By contrast, the PG group of study 2 showed positive correlations between FA and *k* for the left inferior fronto-occipital fascicle and the left superior longitudinal fascicle. Interestingly, when HC and PG groups of study 2 were combined, no significant correlations were observed between *k* and FA pointing to qualitative differences between groups.

Considering the results of the current study, the consistent negative correlation of the left superior longitudinal fascicle, the bilateral inferior longitudinal fascicle and left inferior longitudinal fascicle in healthy non-gamblers in study 1 and 2 could indicate that fiber tracts that transmit frontal control signals, i.e., signals that would counteract the urge to go for the immediate reward, are less prominent in subjects with steeper discounting.

On the other hand, the inferior fronto-occipital fascicle appears to be of particular relevance for PG as it not only emerged in the group comparison HC vs. PG (see below) but also was the only region showing a positive correlation between FA and *k* in PG but a negative correlation in HC. It has to be pointed out that the first effect emerged for the right hemisphere, whereas the latter was found for the left hemisphere. At present, we do not have an explanation for the different laterality of these effects Nevertheless, there appears to be a qualitative difference of the inferior occipito-frontal fascicle between HC and PG groups.

**Table 7** Study 2: Tracts showing a significant decrease of FA in PG (TBSS analysis)

| Brain region | Hemisphere | MNI coordinates | | | Cluster size | *p* (FWE) |
|---|---|---|---|---|---|---|
| | | *X* | *Y* | *Z* | | |
| Superior longitudinal fascicle | R | 36 | 7 | 44 | 327 | 0.02 |
| | R | 45 | 6 | 16 | 498 | 0.02 |
| Superior longitudinal fascicle (temporal part) | L | −50 | −33 | −11 | 251 | 0.02 |
| Inferior longitudinal fascicle | L | −43 | −32 | −12 | 378 | 0.03 |
| Inferior fronto-occipital fascicle | R | 39 | 27 | −7 | 266 | 0.01 |
| Premotor cortex | L | −9 | −17 | 55 | 91 | 0.01 |
| Anterior thalamic radiation | L | −5 | −17 | 9 | 359 | 0.01 |
| Anterior thalamic radiation | R | 11 | −23 | 11 | 295 | 0.01 |

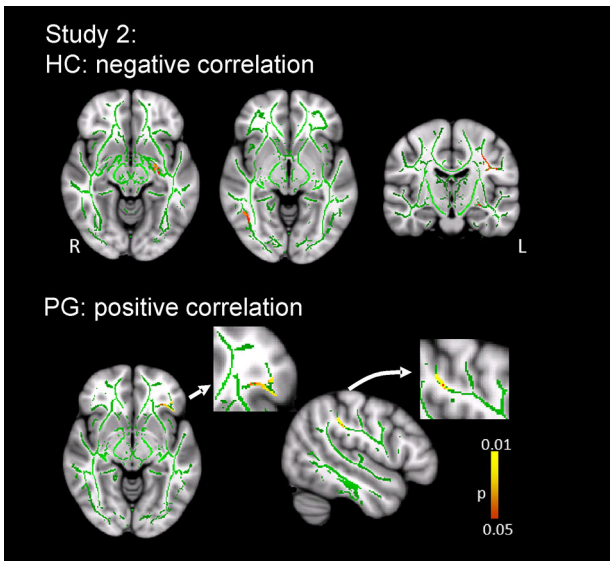


**Fig. 6** Study 2: Relationship of white matter tract FA to the discounting rate *k*. The *k* value was negatively correlated with FA in HC in several white matter tracts (*upper* part of figure, see text) but positively correlated with FA in PG (*lower* part of figure). The *green* voxels show the mean FA skeleton. *Red/yellow* voxels represent regions in which FA was significantly correlated with FA

Based on the dissection of 10 human brain hemisphere and addition DTI studies, Sarubbo et al. (2013) identified different layers and portions of the tract. In particular, the deeper layer could be further subdivided into posterior, middle and anterior portions of which the anterior component was suggested to be involved in emotional and behavioral control aspects. The resolution of the current TBSS analysis is not sufficient to distinguish between the different components of the inferior fronto-occipital fascicle. On the basis of the current data, we suggest that further tractographic analyses into the differences between PG and HC might be most promising to elucidate the neural basis of PG.

## Differences between pathological gamblers and healthy controls

A decreased gray matter volume in PG was evident in right ACC, bilateral SMA, right precentral gyrus, right orbitofrontal cortex, right fusiform gyrus and right inferior temporal gyrus, bilateral insula, right hippocampus, bilateral putamen, and the right amygdala, whereas no brain regions were found showing an increase in gray matter in PG. This data somehow contradict the recent work of Koehler et al. (2013) who reported an increase of gray matter in the right middle frontal gyrus, right subcallosal gyrus, left inferior frontal gyrus and left middle frontal gyrus for PG, whereas no area showed decreased gray matter in PG in this study. In addition, after small volume correction, these authors also found increased local gray matter volume in the right ventral striatum and in the right middle frontal gyrus. A further study by Joutsa et al. (2011) which compared 12 PG to 12 control participants did not find any gray matter volume differences.

Weng et al. (2013) investigated individuals with online game addiction and found a reduction of gray matter in the right orbitofrontal cortex, bilateral insula and right SMA, a pattern which is similar to the one found in the present study.

At present, we are unable to pinpoint the reasons for the differences between the current study and Weng et al. (2013) to the study of Koehler et al. (2013). Some of the areas found by us and Weng et al. (2013), such as the ACC and SMA have been associated with cognitive control and conflict monitoring, suggesting that brain areas related to cognitive control are less well developed in PG which in turn might contribute to the condition. Because of the considerable variability between the different studies (Joutsa et al. 2011; Koehler et al. 2013; current study), any firm conclusion must await further studies in larger cohorts carefully matched for nicotine, alcohol and drug consumption as well as other factors.

With regard to white matter tracts, the current study showed significantly reduced FA in PG in the superior longitudinal fascicle, inferior longitudinal fascicle, inferior fronto-occipital fascicle and the anterior thalamic radiation, while no regions were found showing an increased FA in PG. Some of these findings have also been reported by Joutsa et al. (2011) such as a reduced FA in the anterior thalamic radiation, the inferior longitudinal fascicle,

**Table 8** Study 2: Tracts showing a significant correlation between FA density and *K* value

| Brain region | Hemisphere | MNI coordinates | | | Cluster size | *p* (FWE) |
|---|---|---|---|---|---|---|
| | | *X* | *Y* | *Z* | | |
| PG positive correlation | | | | | | |
| Inferior fronto-occipital fascicle | L | −35 | 32 | −5 | 161 | 0.01 |
| Superior longitudinal fascicle | L | −48 | −36 | 35 | 216 | 0.01 |
| HC negative correlation | | | | | | |
| Superior longitudinal fascicle | L | −37 | −15 | 32 | 296 | 0.01 |
| Inferior longitudinal fascicle | R | 44 | −54 | −5 | 69 | 0.01 |
| Inferior longitudinal fascicle | L | −25 | −14 | −10 | 59 | 0.01 |

superior longitudinal fasciculus and inferior fronto-occipital fasciculus. Yip et al. (2013) also showed a reduced fractional anisotropy in the genu of the corpus callosum in PG. Joutsa et al. (2011) point out that similar changes have also been seen in substance abuse disorders (e.g., Lim et al. 2008; Xu et al. 2010). Further, the superior longitudinal fascicle (Lim et al. 2008; Ashtari et al. 2009; Jacobus et al. 2009; Pfefferbaum et al. 2009; Yeh et al. 2009; Lane et al. 2010; Xu et al. 2010), the inferior longitudinal fascicle (Jacobus et al. 2009; Yeh et al. 2009) and the inferior fronto-occipital fascicle (Yeh et al. 2009) have been seen in previous DTI studies pointing to a general susceptibility to addictions for subjects presenting with a reduced FA in these tracts. Studies in behavioral addictions such as the current one are particularly relevant, as the white matter changes in this case cannot exclusively be explained by direct effects of substances on white matter. In fact, all our participants were screened for a history of substance abuse disorders (except for nicotine), and subjects presenting a history of drug/alcohol abuse and drug treatment with psychotropic medication were excluded. Nicotine use was matched between PG and control subjects.

Fiber tracts such as the superior longitudinal fascicle and the inferior longitudinal fascicle might transmit control signals issued by frontal cortical areas to overcome the urge to go for rewards. Less well-developed WM tracts may thus contribute to pathological gambling.

### Limitations

The current study is one of the first to investigate aspects of gray and white matter anatomy in relation to intertemporal choice and pathological gambling. Whereas sample size in study 1 is well sufficient, group sizes in study 2 are somewhat smaller. Therefore, further morphometric investigations of PG should be performed on larger samples. Furthermore, while the specific method of analysis of white matter tracts (TBSS) reduces the number of statistical tests performed, it also suffers from a lack of spatial selectivity. Fiber tracts like the inferior occipito-frontal fascicle can be subdivided into different portions and layers with different origin and target areas (Sarubbo et al. 2013). Therefore, future studies need to employ finer-grained analyses to pinpoint the white matter tract regions and properties related to impulsivity, as reflected by intertemporal choice behavior, and pathological gambling.

Finally, PG subjects and matched HCs present a considerable daily alcohol and cigarette consumption. Thus, the association between brain structures and $k$ values might be also modulated by alcohol/nicotine use in both groups.

## Conclusions

The present study demonstrates that interindividual differences in intertemporal choice as an indicator of impulsive vs. reflexive choice can be at least partially explained by differences in individual anatomy of both gray and white matter as consistent relationships between the volume of specific brain regions and white matter tracts to the delay discounting parameter $k$ could be observed in three independent groups. While there were a number of previous studies on morphological differences between HC and PG, the novel aspect of the current study is that it establishes the relationship between the steepness of the discounting function, a core aspect of the psychopathology of pathological gambling (Wiehler and Peters 2014) and brain morphology.

Two important novel results emerged with regard to white matter integrity: First, there was a negative correlation of $k$ with the left superior longitudinal fascicle, the bilateral inferior longitudinal fascicle and left inferior longitudinal fascicle in HC in both studies indicating that fiber tracts probably involved in cognitive control are less well developed in people with steeper discounting. Second, the inferior fronto-occipital fascicle showed differences between HC and PG and, furthermore, showed a positive correlation between FA and $k$ in PG but a negative correlation in HC. Thus, this fiber tract appears to be of major importance for pathological gambling. In contrast to the results for the white matter, which replicated most of the previously seen differences between HC and PG, the gray matter findings of the current study show discrepancies to other studies and therefore should be replicated before firm conclusions can be drawn.

Finally, another important way to demonstrate the relevance of certain brain areas and white matter tracts for delay discounting would be the combined analysis of morphometric and functional MRI data. Such functional data are available for the participants of study 2. Indeed, our group has previously shown that intensity of functional activations to rewarding stimuli are partially predicted by white matter integrity (Camara et al. 2010) underscoring the feasibility of such an analysis.

**Acknowledgments** TFM and MH are supported by grants of the DFG and BMBF.

## References

Alessi SM, Petry NM (2003) Pathological gambling severity is associated with impulsivity in a delay discounting procedure. Behav Process 64:345–354

Amiez C, Joseph JP, Procyk E (2006) Reward encoding in the monkey anterior cingulate cortex. Cereb Cortex 16:1040–1055

Andersson JLR, Jenkinson M, Smith S (2007a) Non-linear optimisation. FMRIB technical report TR07JA1 from www.fmrib.ox.ac.uk/analysis/techrep

Andersson JLR, Jenkinson M, Smith S (2007b) Non-linear registration, aka Spatial normalization. FMRIB technical report TR07JA2 from www.fmrib.ox.ac.uk/analysis/techrep

Anokhin AP, Golosheykin S, Grant JD, Heath AC (2011) Heritability of delay discounting in adolescence: a longitudinal twin study. Behav Genet 41:175–183

Ashburner J, Friston K (2000) Voxel-based morphometry—the methods. NeuroImage 11:805–821

Ashtari M, Cervellione K, Cottone J, Ardekani B, Sevy S, Kumra S (2009) Diffusion abnormalities in adolescents and young adults with a history of heavy cannabis use. J Psychiat Res 43:189–204

Basser PJ, Jones DK (2002) Diffusion-tensor MRI: theory, experimental design and data analysis: a technical review. NMR Biomed 15:456–467

Beaulieu C (2002) The basis of anisotropic water diffusion in the nervous system: a technical review. NMR Biomed 15:435–455

Brevers D, Cleeremans A, Verbruggen F, Bechara A, Kornreich C, Verbanck P, Noël X (2012) Impulsive action but not impulsive choice determines problem gambling severity. PLoS One 7:e50647

Camara E, Rodriguez-Fornells A, Münte TF (2010) Microstructural brain differences predict functional hemodynamic responses in a reward processing task. J Neurosci 30:11398–11402

Cho SS, Pellecchia G, Aminian K, Ray N, Segura B, Obeso I, Strafella AP (2013) Morphometric correlation of impulsivity in medial prefrontal cortex. Brain Topogr 26:479–487

Dixon MR, Marley J, Jacobs EA (2003) Delay discounting by pathological gamblers. J Appl Behav Anal 36:449–458

Dixon MR, Jacobs EA, Sanders S (2006) Contextual control of delay discounting by pathological gamblers. J Appl Behav Anal 39:413–422

Frederick S, Loewenstein G, O'Donoghue T (2002) Time discounting and time preference: a critical review. J Economic Lit 40:351–401

Frederick S, Loewenstein G, O'Donoghue T (2003) Time discounting and time preference: A critical review. In: Loewenstein G, Read D, Baumeister R (eds) Time and decision: economic and psychological perspectives on intertemporal choice. Sage, New York, pp 13–86

Good C, Johnsrude I, Ashburner J, Henson R, Friston K, Frackowiak R (2001) A voxel-based morphometric study of ageing in 465 normal adult human brains. NeuroImage 14:21–36

Grant JE, Potenza MN (2004) Pathological gambling: a clinical guide to treatment. American Psychiatric Publishing Inc, Washington, DC

Jacobus J, McQueeny T, Bava S, Schweinsburg B, Frank L, Yang T, Tapert S (2009) White matter integrity in adolescents with histories of marijuana use and binge drinking. Neurotox Teratol 31:349–355

Jenkinson M, Smith SM (2001) A global optimisation method for robust affine registration of brain images. Med Image Anal 5:143–156

Jenkinson M, Bannister PR, Brady JM, Smith SM (2002) Improved optimisation for the robust and accurate linear registration and motion correction of brain images. NeuroImage 17:825–841

Joutsa J, Saunavaara J, Parkkola R, Niemelä S, Kaasinen V (2011) Extensive abnormality of brain white matter integrity in pathological gambling. Psychiatry Res 194:340–346

Kalenscher T, Pennartz CMA (2008) Is a bird in the hand worth two in the future? The neuroeconomics of intertemporal decision-making. Prog Neurobiol 84:284–315

Kalenscher T, Windmann S, Diekamp B, Rose J, Güntürkün O, Colombo M (2005) Single units in the pigeon brain integrate reward amount and time-to-reward in an impulsive choice task. Curr Biol 15:594–602

Kirby KN, Petry NM, Bickel WK (1999) Heroin addicts have higher discount rates for delayed rewards than non-drug-using controls. J Exp Psychol Gen 128:78–87

Koehler S, Hasselmann E, Wüstenberg T, Heinz A, Romanczuk-Seiferth N (2013) Higher volume of ventral striatum and right prefrontal cortex in pathological gambling. Brain Struct Funct **[Epub ahead of print]**

Kräplin A, Dshemuchadse M, Behrendt S, Scherbaum S, Goschke T, Bühringer G (2014) Dysfunctional decision-making in pathological gambling: pattern specificity and the role of impulsivity. Psychiatry Res 215:675–682

Kuhnen CM, Knutson B (2005a) The neural basis of financial risk taking. Neuron 47:763–770

Kuhnen CM, Knutson B (2005b) The neural basis of financial risk taking. Neuron 47(5):763–770

Lane S, Steinberg J, Ma L, Hasan K, Kramer L, Zuniga E, Narayana P, Moeller F (2010) Diffusion tensor imaging and decision making in cocaine dependence. PloS One 5:e11591

Lesieur HR, Blume SB (1987) The South Oaks Gambling Screen (SOGS): a new instrument for the identification of Pathological gamblers. Am J Psychiat 144:1184–1188

Lim KO, Wozniak JR, Mueller BA, Franc DT, Specker SM, Rodriguez CP, Silverman AB, Rotrosen JP (2008) Brain macrostructural and microstructural abnormalities in cocaine dependence. Drug Alcohol Depend 92:164–172

Marco-Pallares J, Mohammadi B, Samii A, Münte TF (2010) Brain activations reflect individual discount rates in intertemporal choice. Brain Res 1320:123–129

Mazur JE (1984) Tests of an equivalence rule for fixed and variable reinforcer delays. J Exp Psychol Anim Behav Process 10:426–436

McClure SM, Laibson DI, Loewenstein G, Cohen JD (2004) Separate neural systems value immediate and delayed monetary rewards. Science 306:503–507

Miedl SF, Fehr T, Meyer G, Herrmann M (2010) Neurobiological correlates of problem gambling in a quasi-realistic blackjack scenario as revealed by fMRI. Psychiatry Res 181:165–173

Miedl SF, Peters J, Büchel C (2012) Altered neural reward representations in pathological gamblers revealed by delay and probability discounting. Arch Gen Psychiatry 69:177–186

Milenkova M, Mohammadi B, Kollewe K, Schrader C, Fellbrich A, Wittfoth M, Dengler R, Münte TF (2011) Intertemporal choice in Parkinson's disease. Mov Disord 26:2004–2010

Mitchell SH (1999) Measures of impulsivity in cigarette smokers and non-smokers. Psychopharmacology 146:455–464

Mitchell JM, Fields HL, D'Esposito M, Boettiger CA (2005) Impulsive responding in alcoholics. Alcohol Clin Exp Res 29:2158–2169

Papadakis NG, Xing D, Huang CL, Hall LD, Carpenter TA (1999) A comparative study of acquisition schemes for diffusion tensor imaging using MRI. J Magn Reson 137:67–82

Peper JS, Mandl RCW, Braams BR, de Water E, Heijboer AC, Koolschijn PCMP, Crone EA (2013) Delay discounting and frontostriatal fiber tracts: a combined DTI and MTR study on impulsive choices in healthy young adults. Cerebral Cortex 23:1695–1702

Peters J, Büchel C (2011) The neural mechanisms of inter-temporal decision-making: understanding variability. Trends Cogn Sci 15:227–239

Petry J (1996) Psychotherapie der Glücksspielsucht. Beltz, Weinheim

Petry NM (2001a) Delay discounting of money and alcohol in actively using alcoholics, currently abstinent alcoholics, and controls. Psychopharmacology 154:243–250

Petry NM (2001b) Pathological gamblers, with and without substance use disorders, discount delayed rewards at high rates. J Abnorm Psychol 110:482–487

Pfefferbaum A, Rosenbloom M, Rohlfing T, Sullivan EV (2009) Degradation of association and projection white matter systems in alcoholism detected with quantitative fiber tracking. Biol Psychiat 65:680–690

Preuschoff K, Quartz SR, Bossaerts P (2008) Human insula activation reflects risk prediction errors as well as risk. J Neurosci 28:2745–2752

Reynolds B, Richards JB, Horn K, Karraker K (2004) Delay discounting and probability discounting as related to cigarette smoking status in adults. Behav Processes 65:35–42

Rolls ET (2004) The functions of the orbitofrontal cortex. Brain Cogn 55:11–29

Rueckert D, Sonoda LI, Hayes C, Hill DL, Leach MO, Hawkes DJ (1999) Nonrigid registration using free-form deformations: application to breast MR images. IEEE Trans Med Imaging 18:712–721

Sarubbo S, De Benedictis A, Maldonado IL, Basso G, Duffau H (2013) Frontal terminations for the inferior fronto-occipital fascicle: anatomical dissection, DTI study and functional considerations on a multi-component bundle. Brain Struct Funct 218:21–37

Skare S, Hedehus M, Moseley ME, Li TQ (2000) Condition number as a measure of noise performance of diffusion tensor data acquisition schemes with MRI. J Magn Reson 147:340–352

Smith S (2002) Fast robust automated brain extraction. Hum Brain Mapp 17:143–155

Smith S, Nichols T (2009) Threshold-free cluster enhancement: addressing problems of smoothing, threshold dependence and localisation in cluster inference. NeuroImage 44:83–98

Smith SM, Jenkinson M, Woolrich MW, Beckmann CF, Behrens TE, Johansen-Berg H, Bannister PR, De Luca M, Drobnjak I, Flitney DE, Niazy RK, Saunders J, Vickers J, Zhang Y, De Stefano N, Brady JM, Matthews PM (2004) Advances in functional and structural MR image analysis and implementation as FSL. Neuroimage 23(Suppl 1):S208–S219

Smith SM, Jenkinson M, Johansen-Berg H, Rueckert D, Nichols TE, Mackay CE, Watkins KE, Ciccarelli O, Cader MZ, Matthews PM, Behrens TE (2006) Tract-based spatial statistics: voxelwise analysis of multi-subject diffusion data. Neuroimage 31:1487–1505

Waxman SG, Bennett MV (1972) Relative conduction velocities of small myelinated and non-myelinated fibres in the central nervous system. Nat New Biol 238:217–219

Weng CB, Qian RB, Fu XM, Lin B, Han XP, Niu CS, Wang YH (2013) Gray matter and white matter abnormalities in online game addiction. Eur J Radiol 82:1308–1312

Wiehler A, Peters J (2014) Reward-based decision making in pathological gambling: the roles of risk and delay. Neurosci Res. doi:10.1016/j.neures.2014.09.008

Wittchen H-U, Zaudig M, Fydrich T (1997) Strukturiertes Klinisches Interview für DSM-IV. Hogrefe, Göttingen

Xu J, DeVito EE, Worhunsky PD, Carroll KM, Rounsaville BJ, Potenza MN (2010) White matter integrity is associated with treatment outcome measures in cocaine dependence. Neuropsychopharmacology 35:1541–1549

Xue G, Lu Z, Levin IP, Bechara A (2010) The impact of prior risk experiences on subsequent risky decision-making: the role of the insula. NeuroImage 50:709–716

Yeh PH, Simpson K, Durazzo TC, Gazdzinski S, Meyerhoff DJ (2009) Tract-Based Spatial Statistics (TBSS) of diffusion tensor imaging data in alcohol dependence: abnormalities of the motivational neurocircuitry. Psychiatry Res 173:22–30

Yip SW, Lacadie C, Xu J, Worhunsky PD, Fulbright RK, Constable RT, Potenza MN (2013) Reduced genual corpus callosal white matter integrity in pathological gambling and its relationship to alcohol abuse or dependence. World J Biol Psychiatry 14:129–138

Zhang Y, Brady M, Smith S (2001) Segmentation of brain MR images through a hidden Markov random field model and the expectation maximization algorithm. IEEE Trans Med Imaging 20:45–57